ACS Combinatorial Science

Research Article

pubs.acs.org/acscombsci

High-Throughput Measurement of Ionic Conductivity in Composition-Spread Thin Films

H. Duan,*,† C. C. Yuan, N. Becerra, L. J. Small, A. Chang, J. M. Gregoire, and R. B. van Dover

Department of Materials Science and Engineering, Cornell University, Ithaca, New York 14853, United States

Supporting Information

ABSTRACT: This paper demonstrates the feasibility of high-throughput investigation of ionic conductivity in oxygen-ion conductors. Yttria stabilized zirconia (YSZ) composition-spread thin films with nanometer-size grains were prepared by 90° off-axis reactive RF cosputtering. We compare results for two electrode configurations, namely, out-of-plane (parallel plate) and in-plane (planar interdigitated electrode) and find that the contribution from the intragrain conductivity in YSZ thin films (150 nm) is more explicit in the latter configuration because it greatly diminishes electrode effects. The intragrain oxygen ion conductivity of thin film YSZ was systematically measured as a function of yttria concentration over the range 2 mol % to 12 mol %. The results show that the measured conductivity of the YSZ thin films is close to that of corresponding bulk materials with a peak value around 3×10^{-4} S cm^{-1} at 440 °C at the optimum Y_2O_3 concentration of 8 mol %. Validation of this technique means that it can be applied to novel chemical systems for which systematic bulk measurements have not been attempted.

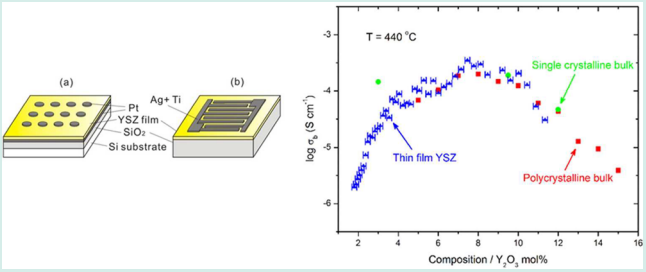

KEYWORDS: *yttria-stabilized zirconia thin films, composition-spread, cosputtering, ionic conductivity*

INTRODUCTION

Intensive study has been carried out on nanostructured yttria-stabilized zirconia (YSZ) thin films in recent years with two main goals: (1) studying space-charge effects[1] on the electrical conduction when one of the sample dimensions is comparable to the Debye length; and (2) evaluating suitability as the electrolyte material for intermediate (650−800 °C) or low temperature (≤650 °C) micro solid oxide fuel cells (SOFCs)[2,3] or sensors.[4] Ionic conductivity is the primary measure of performance for an ionic conductor. However, the reported ion conductivity data of YSZ films with nanometer thickness are inconclusive. Karthikeyan et al. fabricated the film by electron beam evaporation and observed a monotonic increase of conductivity with decreasing thickness in the range of 17−210 nm.[1] Kosacki et al. used pulsed laser deposition (PLD) to deposit the YSZ film, reported exceptionally high ionic conductivity when the film thickness was less than 60 nm, and attributed it to a significant contribution from interface conductivity.[5] In contrast, Gerstl et al. found that the intragrain conductivity of YSZ thin films (18 and 32 nm) deposited by PLD was close to that of bulk specimens.[6] Kim et al. also reported no conductivity enhancement for RF sputtered YSZ films that were 180, 360, and 900 nm thick.[7]

Impedance spectroscopy is widely used to infer ionic conductivity using one of two basic electrode geometries, namely, out-of-plane[8−10] and in-plane[1,5−7,9,11] configuration. In the former configuration, the YSZ film is sandwiched between top and bottom metal electrodes; and while current flows perpendicular to the film plane during measurement in the same manner as in an operational SOFC, the measurement may be strongly affected by the close spacing of the electrodes. In the in-plane configuration, both electrodes are deposited on top of the YSZ film; since the interelectrode spacing is typically ∼5−10 μm, the electrodes have much less influence on ion conduction.

In this paper we compare and evaluate the two electrode configurations using YSZ thin films with thickness ∼150 nm. We also report the dependence of the intragrain conductivity on Y_2O_3 concentration using the cosputtered composition spread approach, a powerful and versatile method for the efficient study of a wide range of compositions with excellent compositional resolution.[12]

EXPERIMENTAL PROCEDURES

Composition-Spread Preparation. YSZ composition-spread thin films were deposited on unheated substrates by 90° off-axis reactive RF cosputtering using elemental Zr and Y targets. The substrates were either 3″ diameter Si wafers with a 600 nm thick thermally grown SiO_2 layer or 3″ fused silica wafers (Quartz Unlimited LLC.). The sputtering system was operated with a base pressure of 2×10^{-6} Torr and a working pressure of 3×10^{-2} Torr with gas flows of 10 std. cm^3 min^{-1} (sccm) O_2 and 15 sccm Ar. RF powers applied to the Zr target and the Y target were 103 and 50 W, respectively, giving a center composition of approximately $Zr_{0.80}Y_{0.20}O_y$. To obtain

Received: June 19, 2012
Published: May 5, 2013

   dx.doi.org/10.1021/co4000375 | ACS Comb. Sci. 2013, 15, 273−277

dense films, ~ 10 W RF power was applied to the substrate to maintain a −75 V DC bias. A 45 min deposition gave a thickness of 150 nm at the center of the wafer. The films were annealed in air at 500 °C (for out-of-plane measurement films) and 1000 °C (for in-plane measurement films) at a heating rate of 5 °C min^{-1} with a 1 h soak to achieve crystallinity and to preclude significant structural changes during conductivity measurements.

Materials Characterization. The morphology and microstructure of the resulting films were characterized by transmission electron microscopy (TEM, Tecnai F20) and X-ray diffraction (Bruker D8 Discover with GADDS). TEM samples were prepared by manual lapping followed by ion milling to electron transparency using an ion mill (Fischione 1010). Thin film thickness was determined by ellipsometry using an M-2000 Woollam Spectroscopic Ellipsometer. Chemical compositions were measured by wavelength dispersive X-ray spectroscopy (WDS, JEOL 8900 Microprobe) and X-ray photoelectron spectroscopy (XPS, Surface Science Instrument SSX-100) and also calculated using single-cation calibration data (see Supporting Information).

Electrical Measurement. For electrical measurements, two electrode configurations (see Figure 1) were tested, namely, the

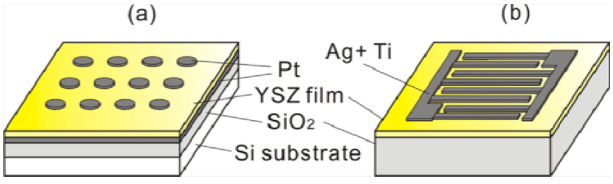

Figure 1. Schematic of (a) out-of-plane configuration and (b) in-plane (interdigitated) configuration for electrical measurements; the IDE footprint was 1 mm × 1 mm.

out-of-plane and in-plane (interdigitated electrode, IDE) geometries. For the former, thermally oxidized Si substrates were used. Before the deposition of YSZ films, a uniform 40 nm thick Pt layer was deposited using electron beam evaporation to serve as the base electrode for all of the parallel-plate capacitors. Ar-ion bombardment was employed during evaporation to promote adhesion of Pt to the substrate. After the YSZ deposition, top electrodes were deposited by evaporating a 35 nm Pt layer through a shadow mask consisting of a square array of 200 μm diameter dots. For the IDE configuration, YSZ was directly deposited on fused-silica substrates; interdigitated electrodes comprising 120 nm Ag and a 20 nm Ti adhesion layer were prepared by electron beam evaporation and photolithographic lift-off (see Figure 1). The finger length, width, and interelectrode spacing were 750 μm, 5 μm, and 5 μm, respectively. IDEs were fabricated on 1 mm centers in an array covering the substrate.

The ionic conductivity of the YSZ composition spreads was evaluated using electrochemical impedance spectroscopy (EIS) measurements in an air atmosphere using an HP 4284 LCR meter with an AC amplitude of 100 mV and frequencies ranging from 100 Hz to 1 MHz (5−10 measurement frequencies per decade). Measurements were carried out at temperatures between 300 and 500 °C using a probe station in which the samples were fixed to a heated plate with silver thermal paste. Temperature readings were calibrated with a thermocouple attached to a fused quartz wafer using silver filled epoxy. The impedance of the bare quartz substrate was measured under the same conditions using interdigitated electrodes; that impedance was determined to be about 1 order of magnitude greater than that of the YSZ film. To measure the out-of-plane devices the common base electrode was contacted using an Au wire attached by silver-filled epoxy, and the counter electrode was contacted using a Pd-needle attached to a micropositioner. For the IDE devices, two Pd-tipped probes on micropositioners were used to make contact to the two electrodes of each device measured. Individual devices were measured sequentially. This measurement scheme could be straightforwardly modified for fully automated data acquisition using an automated probe station.

We note that the physical footprint of the electrode for our in-plane configuration is a 1 × 1 mm^2 square, so the composition of each point in Figure 4 represents an average composition over that area on the composition spread. However, the composition gradient is small (a range of 1.8−11.8 Y_2O_3 mol %, over a span of 75 mm), so that each electrode averages over a composition range of only about 0.5 atom % Y.

RESULTS AND DISCUSSION

Figure 2a shows a bright field TEM image of the cross section of the $Zr_{0.94}Y_{0.06}O_{1.97}$ film. It can be seen that the film is dense

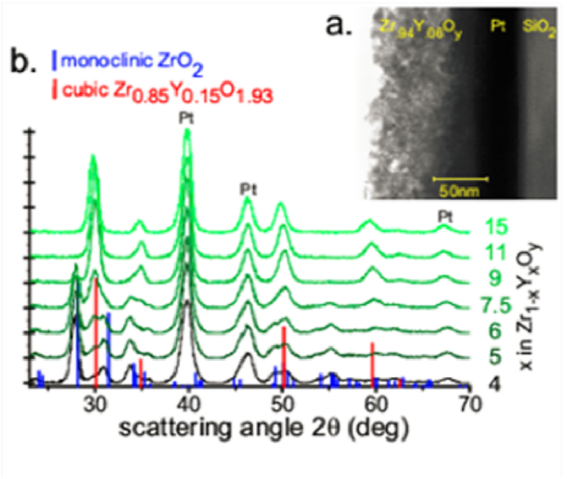

Figure 2. Structural data for the film annealed at 500 °C. Data for the film annealed at 1000 °C are essentially identical. (a) Cross-section TEM image of the YSZ thin film, (b) XRD patterns for the $Zr_{1-x}Y_xO_y$ composition spread.

with no discernible voids or cracks despite the off-axis deposition technique. It needs to be noted that the rough surface of the left edge in Figure 2a is a result of TEM sample preparation. This desirable film morphology is achieved as a result of ion bombardment induced by the substrate bias, without such bias a microstructure with fibrous voids is typically observed.[13] The average grain size is estimated on the order of 10 nm.

Figure 2b shows the XRD patterns as a function of composition in the composition spread, specifically for the film deposited at 500 °C. Composition is a critical parameter and not trivial to determine accurately in a thin film. We have found that, with high reliability: (1) the depositions of ZrO_2 and Y_2O_3 do not interfere with one other during cosputtering and (2) the deposition rate is constant over time, with a negligibly small variation from run to run. These observations are documented in ref 14. We used identical sputtering

dx.doi.org/10.1021/co4000375 | ACS Comb. Sci. 2013, 15, 273−277

parameters to prepare ZrO_2 and Y_2O_3 composition spreads separately and used ellipsometry to determine the thickness at many spots along the symmetry axis. By fitting the thickness using an empirical model (Supporting Information, Figure S1), we get the thickness distribution over the whole composition spread. Then, after considering variables such as density, molecular weight, and deposition time, we infer the deposition rate for each cation. Simple superposition of the deposition rates allows us to calculate the composition of the cosputtered ZrO_2−Y_2O_3 composition spread (Supporting Information, Figure S2). Local measurements (electron microprobe (WDS) and X-ray photoemission) showed agreement with calculated composition values within the error limit of measurement technique.

For each diffraction spectrum the scattering angle scale was corrected using the internal Pt calibration; the same background was subtracted from all patterns. The peaks in Figure 2b, other than those from the Pt underlayer, match well with either monoclinic ZrO_2 (PDF# 00-007-0343) or cubic YSZ (PDF# 00-030-1468) phase. As expected, the phase changes from monoclinic ZrO_2 to cubic $Zr_{1-x}Y_xO_{2-x/2}$ as the Y concentration (x) increases from 4 atom % to 15 atom %. Interestingly, the film was observed to be almost fully cubic for x = 0.09, a value that is significantly less than the Y content required to stabilize the cubic phase of the bulk materials (∼16 atom % Y). The possible reasons, as speculated in ref 11, may include the nanoscale grains, reduced deposition temperatures, and/or substrate induced stresses. Both monoclinic and cubic peaks shift to the lower angle compared to the standard PDF values as a result of the substitution of larger Y^{3+} with Zr^{4+},[15] which increases the $(\bar{1}11)$ d-spacing by up to 2.8%. Peak width analysis using the Scherrer equation reveals an average grain size around 10 nm, which agrees well with the TEM results. X-ray diffraction analysis of the film annealed at 1000 °C showed essentially identical results regarding the stability of the cubic phase. Somewhat surprisingly, annealing at 1000 °C resulted in no measurable increase in the grain size as inferred from the diffraction peak widths. Nevertheless the electrical properties in the two cases are very different, as described below.

For ionic conductivity measurement of the YSZ composition spreads at elevated temperatures, temperature uniformity over the 3″ substrate is of critical importance. The conductivity typically has an Arrhenius dependence: $\sigma_i = (A/T)\ e^{(-E_a/kT)}$, where σ_i is ionic conductivity, A is a material specific constant, T is absolute temperature, k is the Boltzmann's constant, and E_a is the activation energy. For an ion conduction process with activation energy of 1 eV, at 400 °C a change of only 1 °C would produce a relative change of 2.5% in conductivity. We therefore paid careful attention to thermal impedances and confirmed that the substrate temperature uniformity across the wafer was within ±3 °C using a test wafer and calibration thermocouples.

Figure 3 compares the effect of electrode configuration on the Nyquist plots recorded at 440 °C, together with a complex nonlinear least-squares fit of the data to the equivalent circuit shown in the inset. Clearly, electrode configuration has significant impact on the shape of the plots, and in-plane configuration is advantageous over out-of-plane configuration for 150 nm YSZ films in the present work. For out-of-plane configuration, the plot exhibits an arc at high frequencies associated with conduction in the YSZ film and a tail at low frequencies related to the interface between YSZ film and top electrodes.[9,16] For this device the thickness of the YSZ film was

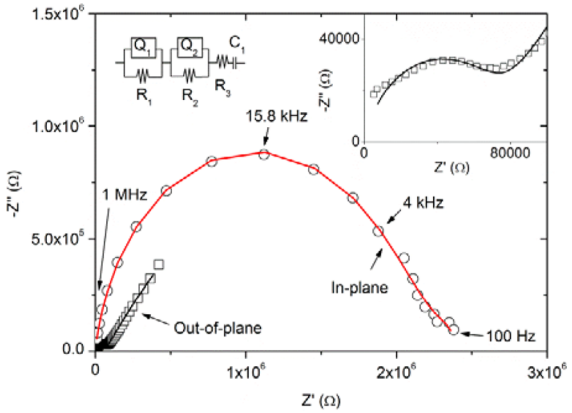

Figure 3. Nyquist impedance plots for thin film $Zr_{0.96}Y_{0.04}O_{1.98}$ with two different electrode configurations. The film measured out-of-plane was heat treated to 500 °C, while the film measured in-plane was heat treated to 1000 °C. Inset: the impedance plot with out-of-plane configuration at high frequencies. The measurement temperature was 440 °C. Points are experimental data; lines are the model fit generated using the inset equivalent circuit.

around 150 nm, which results in a substantial overlap between the high frequency and low frequency responses, preventing achievement of a good fit (inset in Figure 3) that would yield a reliable value for the intragrain ionic conductivity. Essentially, this is due to the inadequate model we have for the low-frequency behavior (it is not a simple series capacitor). At higher temperatures or with thinner YSZ films, the overlapping is even more severe. We note that the out-of-plane configuration has been used successfully for conductivity measurements in YSZ films with thicknesses 10-fold larger (>∼1 μm)[9,16] or at low temperatures (≤300 °C)[9,17] where the low conductivity of the YSZ thin films overwhelms electrode effects. Also, Navickas et al. recently showed that the highly overlapped responses obtained for very thin YSZ films (20−90 nm) with out-of-plane electrodes can be analyzed to reliably infer conductivity data. Their success was apparently made possible by introducing a silica interlayer to prevent pinholes or other adverse interactions with the electrodes.[10]

In-plane measurements using IDEs significantly decrease the electrode effects at frequencies as low as 100 Hz because of the large distance (5 μm) between electrode legs. For the in-plane configuration data shown in Figure 3, the distorted high-frequency semicircle represents overlapped intragrain and intergrain impedance, while the small tail at ∼100 Hz represents the start of electrode effects at the lowest frequency. This contrasts with some reported results for thin film YSZ in which only intragrain contributions were required to describe the data,[9,11,18] possibly because of the small grain size of our YSZ films (Figure 2a). A series connection of two parallel resistor/constant-phase element networks (R_1, R_2, Q_1 and Q_2 in inset of Figure 3) representing the contribution of intragrain and intergrain conduction was required to obtain a good fit for the experiment data. A resistor (denoted R_3 in) and capacitor (denoted C_1) in series were included in the analysis to represent the electrode effects but yielded negligible values as expected. The typical value of the exponent of the constant phase elements corresponding to the intragrain impedance is in the range of 0.95−0.988. In this study we focus on the intragrain conductivity, σ_b, because it exhibits a well-established dependence on Y_2O_3 concentration.[19]

dx.doi.org/10.1021/co4000375 | ACS Comb. Sci. 2013, 15, 273−277

The annealing temperature for the sample used for out-of-plane measurements was 500 °C while the annealing temperature for the sample used for in-plane measurements was 1000 °C. Even though the structure and grain size of the two films were essentially identical, the films annealed at 500 °C were found to have dramatically lower intragrain conductivity than those annealed at 1000 °C. We speculate that the difference is due to improved crystallographic order in the high-temperature-annealed film, which might be elucidated by refined structural comparison of the two films. In any case we have focused on the electrical characterization of the high-temperature-annealed film measured with IDEs, since this data allows the most robust interpretation.

Figure 4 presents the intragrain ionic conductivities of the YSZ film measured at 440 °C as a function of mol % Y_2O_3. The

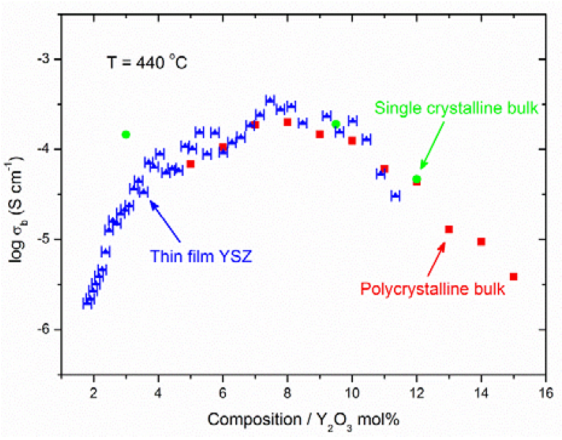

Figure 4. Intragrain ionic conductivity as a function of Y_2O_3 concentration of the YSZ composition spread (hollow triangle) for a film annealed at 100 °C and measured at 440 °C. Literature values for the polycrystalline (filled square[15]) and single crystalline (filled circle[20]) bulk YSZ are given for comparison.

intragrain conductivity,σ_b, is given by $\sigma_b = D/(R_b \times L \times t)$, where R_b is the measured (fitted) intragrain resistance, D is the distance between the IDE legs, L is the cumulative length of the IDE legs, and t is the YSZ thickness. For comparison, the ionic conductivities reported for both polycrystalline[15] and single crystalline[20] bulk YSZ samples at 440 °C are interpolated and plotted. The intragrain conductivities we infer for our composition-spread YSZ thin film show essentially identical values and trend with Y_2O_3 content. The peak conductivity is approximately 3×10^{-4} S cm^{-1} at 440 °C, and the optimal Y_2O_3 concentration is close to 8 mol %. Our results are consistent with reports that single-composition (8 mol % Y_2O_3–ZrO_2 thin films with thicknesses ranging from 18 nm to 1.5 μm prepared by RF sputtering[7] and PLD[6,9] have conductivities close to the bulk samples with the same composition in the temperature range of 200 to 800 °C. The present results demonstrate that similar congruence is obtained over a wide range of Y_2O_3 concentrations, from 2 mol % to 12 mol %, measured at 440 °C. We note that films described in ref 11 were prepared using a reactive magnetron sputtering technique but different experiment process (different working pressure, argon to oxygen ratio, film thickness, postdeposition process, and gun-substrate configuration), and that the films exhibited an unexpected enhancement of ionic conductivity. This, along with our observation of the anomalously low conductivity for our 500 °C-annealed films, shows that close attention to process conditions is necessary to generate results that are representative of the bulk.

CONCLUSION

This work demonstrates that reliable measurements of ionic conductivity can be made using codeposited composition-spread thin films, in that the measurements yield values that are consistent with the intragain conductivity reported for bulk samples. This approach allows high-throughput measurement of behavior over a wide range of compositions with 0.5 atom % resolution in multication oxide systems. We used YSZ as a model system, varying the yttria concentration over the range 2 mol % to 12 mol % Y_2O_3. The in-plane electrode configuration was found to be more suitable than out-of-plane configuration for measurements on 150 nm films. The intragrain ionic conductivity of the YSZ thin films is essentially identical to that of bulk specimens, with a peak conductivity value of about 3×10^{-4} S cm^{-1} at 440 °C for the optimum Y_2O_3 concentration near 8 mol %.

ASSOCIATED CONTENT

Supporting Information

Detailed description of composition determination of the composition spread. This material is available free of charge via the Internet at http://pubs.acs.org.

AUTHOR INFORMATION

Corresponding Author

*Phone: (86) 21-34202549. Fax: (86) 21-34202549. E-mail: hd83@cornell.edu.

Present Address

†(H.D.): 331 Materials Building D, Shanghai Jiao Tong University, 800 Dongchuan Rd, Minhang district, Shanghai, China 200240.

Funding

This research was supported by the U.S. Department of Energy (DOE) Office of Basic Energy Sciences under Award Number DE-FG02−07ER46440.

Notes

The authors declare no competing financial interest.

ACKNOWLEDGMENTS

This work utilized XRD and TEM facilities of the Cornell Center for Materials Research (NSF Funding: DMR-0520404), and was performed in part at the Cornell NanoScale Facility, a member of the National Nanotechnology Infrastructure Network, which is supported by the National Science Foundation (Grant ECS-0335765).

REFERENCES

(1) Karthikeyan, A.; Chang, C. L.; Ramanathan, S. High temperature conductivity studies on nanoscale yttria-doped zirconia thin films and size effects. *Appl. Phys. Lett.* **2006**, *89*, 183116.

(2) Beckel, D.; Bieberle-Hütter, A.; Harvey, A.; Infortuna, A.; Muecke, U. P.; Prestat, M.; Rupp, J. L. M.; Gauckler, L. J. Thin films for micro solid oxide fuel cells. *J. Power. Sources* **2007**, *173*, 325−345.

(3) Kerman, K.; Lai, B. K.; Ramanathan, S. Free standing oxide alloy electrolytes for low temperature thin film solid oxide fuel cells. *J. Power Sources* **2012**, *202*, 120−125.

(4) Yu, S.; Wu, Q.; Tabib-Azar, M.; Liu, C. Development of a silicon-based yttria-stabilized-zirconia (YSZ), amperometric oxygen sensor. *Sens. Actuators B* **2002**, *85*, 212−218.

(5) Kosacki, I.; Rouleau, C. M.; Becher, P. F.; Bentley, J.; Lowndes, D. H. Nanoscale effects on the ionic conductivity in highly textured YSZ thin films. *Solid State Ionics* **2005**, *176*, 1319−1326.
(6) Gerstl, M.; Navickas, E.; Friedbacher, G.; Kubel, F.; Ahrens, M.; Fleig, J. The separation of grain and grain boundary impedance in thin yttria stabilized zirconia (YSZ) layers. *Solid State Ionics* **2011**, *185*, 32−41.
(7) Kim, S. M.; Son, J. W.; Lee, K. R.; Kim, H.; Kim, H. R.; Lee, H. W.; Lee, J. H. Substrate effect on the electrical properties of sputtered YSZ thin films for co-planar SOFC applications. *J. Electroceram.* **2010**, *24*, 153−160.
(8) Brahim, C.; Ringuede, R.; Cassir, M.; Putkonen, M.; Niinisto, L. Electrical properties of thin yttria-stabilitzed zirconia overlayers produced by atomic layer deposition for solid oxide fuel cell applications. *Appl. Surf. Sci.* **2007**, *253*, 3962−3968.
(9) Joo, J. H.; Choi, G. M. Electrical conductivity of YSZ film grown by pulsed laser deposition. *Solid State Ionics* **2006**, *177*, 1053−1057.
(10) Navikas, E.; Gerstl, M.; Friedbacher, G.; Kubel, F.; Fleig, J. Measurement of the across-plane conductivity of YSZ thin films on silicon. *Solid State Ionics* **2012**, *211*, 58−64.
(11) Jung, W. C.; Hertz, J. L.; Tuller, H. L. Enhanced ionic conductivity and phase meta-stability of nano-sized thin film yttria-doped zirconia (YDZ). *Acta Mater.* **2009**, *57*, 1399−1404.
(12) van Dover, R. B.; Schneemeyer, L. F. The codeposited composition spread approach to high-throughput discovery/exploration of inorganic materials. *Macromol. Rapid Commun.* **2004**, *25*, 150−57.
(13) Barron, S. C.; Noginov, M. M.; Werder, D.; Schneemeyer, L. F.; van Dover, R. B. Dielectric response of tantalum oxide subject to induced ion bombardment during oblique sputter deposition. *J. Appl. Phys.* **2009**, *106*, 104110.
(14) Gregorie, M.; Dale, D.; Kazimirov, A.; DiSalvo, F. J.; van Dover, R. B. Cosputtered composition-spread reproducibility established by high-throughput x-ray fluorescence. *J. Vac. Sci. Technol. A* **2010**, *28*, 1279−1280.
(15) Arachi, Y.; Sakai, H.; Yamamoto, O.; Takeda, Y.; Imanishai, N. Electrical conductivity of the ZrO_2 $-Ln_2O_3$ (Ln = lanthanides) System. *Solid State Ionics* **1999**, *121*, 133−139.
(16) Briois, P.; Gourba, E.; Billard, A.; Ringuede, A.; Cassir, M. Microstructure - electrical properties relationship of YSZ thin films reactively sputter-deposited at different pressures. *Ionics* **2005**, *11*, 301−305.
(17) River, A.; Santamaria, J.; Leon, C. Electrical conductivity relaxation in thin-film yttria-stabilitzed zirconia. *Appl. Phys. Lett.* **2001**, *78*, 610−612.
(18) Sillassen, M.; Eklund, P.; Sridharan, M.; Pryds, N.; Bonanos, N.; Bottiger, J. Ionic conductivity and thermal stability of magnetron-sputtered nanocrystalline yttria-stabilized zirconia. *J. Appl. Phys.* **2009**, *105*, 104907.
(19) Luo, J.; Almond, D. P.; Stevens, R. Ionic mobilities and association energies from an analysis of electrical impedance of ZrO_2−Y_2O_3 alloys. *J. Am. Ceram. Soc.* **2000**, *83*, 1703−1708.
(20) Filal, M.; Petot, C.; Mokchah, M.; Chateau, C.; Carpentier, J. L. Ionic conductivity of yttrium-doped zirconia and the "composite effect. *Solid State Ionics* **1995**, *80*, 27−35.